An Uncertainty-Based Voltage Control Model of a Smart Active Network in the Presence of Electric Vehicles: A Distributed Optimization Approach

Mahla Nazari [1*], Saeid Esmaeili [1], Mojtaba Barkhordari Yazdi [1]

[1] Electrical Engineering Department, Shahid Bahonar University of Kerman, Kerman, Iran

∗ nazarimahla97@gmail.com

Abstract: Nowadays, Distributed Energy Resources (DERs) and Electric Vehicles (EVs) are being increasingly used in smart distribution networks. There are concerns regarding the use of DERs and EVs which are twofold: (i) they may lead to grid voltage variation and (ii) they have uncertainty in power production. In this paper, a distributed voltage control method is proposed in the simultaneous presence of DERs and EVs preserving the independence and reducing the communications between them while considering probabilistic behaviors. The proposed objective function improves the system voltage profile with the lowest rate of change in the active and reactive power of DERs and EVs. For this purpose, a method is developed for converting the centralized optimization problem to the distributed optimization problem using Dual-Decomposition (DD) and Alternating Direction Method of Multipliers (ADMM) algorithms based on Peer-to-Peer (P2P) communication capabilities of DERs and EVs. The uncertainty of DERs and EVs are modelled by utilizing a scenario-based approach and a Two-Point Estimation Method (2PEM), respectively. The results on the modified IEEE 69-bus test system show that the proposed method can improve the voltage deviation of the worst bus by about 7%, and also reduce grid losses by about 48%.

Keywords: Distributed optimization, Alternating direction method of multipliers (ADMM), Distributed energy resources (DERs), Electric vehicles (EVs), Uncertainty.

Nomenclature

Indices

t	Index of time slot
n, j	Index of distribution network buses
p	Index of parking lots
k	Index of DD and ADMM iteration
d	The number of smart photovoltaic inverters
L	Lines between n, j buses

Parameters

c_d^P	Penalty factor to control active power changes
c_d^Q	Penalty factor to control reactive power changes
c_p^P	Penalty factor to control changes in the active discharge power of EVs
V_{nom}	Nominal network voltage (p.u)
V_{max}	Maximum network voltage
V_{min}	Minimum network voltage
$R_{d,i}$	Lines resistance
$X_{d,i}$	Lines reactance
ρ	ADMM algorithm convergence acceleration factor
α	DD algorithm convergence acceleration factor
$\Delta P_{max,d}$	Maximum active power changes of each inverter
$\Delta P_{min,d}$	Minimum active power changes of each inverter
$\Delta Q_{max,d}$	Maximum reactive power changes of each inverter
$\Delta Q_{min,d}$	Minimum reactive power changes of each inverter
$\Delta P_{max,p}$	Maximum changes in the active discharge power of EVs
$\Delta P_{min,p}$	Minimum changes in the active discharge power of EVs
ε_{thr}	Convergence threshold
$P_{d,0}$	Active power set point before applying the changes
$Q_{d,0}$	Reactive power set point before applying the changes
$P_{p,0}$	Active discharge power set point before applying the changes

Variables

$V_{n,0}$	The voltage of each bus before applying the changes
$V_{n,t}$	The voltage of each bus
$P_{(n,j)}^{Loss}$	Active power losses
$P_{(n,j)}^{T,Loss}$	Total network power losses
$P_{d,t}$	Active power of each inverter after applying changes
$Q_{d,t}$	Reactive power of each inverter after applying changes
$P_{p,t}$	Active power of EVs discharge after applying changes
$\lambda_{n,t}^{max}$	Lagrangian multiplier related to the maximum voltage inequality constraint
$\lambda_{n,t}^{min}$	Lagrangian multiplier related to the minimum voltage inequality constraint
$\Delta P_{d,t}$	Active power changes of each smart inverter
$\Delta Q_{d,t}$	Reactive power changes of each smart inverter
$\Delta P_{p,t}$	Active discharge power changes of EVs

1. Introduction

The development of Distributed Energy Resources (DERs) encourages communities to play a role in smart

networks. The rapid growth of penetration of DERs in the power system helps to supply electrical energy

needs without increasing fossil fuel consumption, and it also greatly reduces the emission of greenhouse

gases [1]. In addition to the presence of renewable energy resources such as wind and solar sources in the

network, Electric Vehicles (EVs) also are used, which are a new and growing technology in smart networks [2,3]. EVs help to reduce pollution [4] and also its connection to the network improves reliability [5]. Increasing the number of EVs in smart networks leads to an increase in network energy demand, as well as current harmonics. In the absence of management on the pattern of receiving their energy from the network, the voltage of the buses and the loading of the lines may be out of range. For this purpose, active and reactive power management of EVs is done by using bidirectional chargers to minimize voltage deviation [6]. In [7], also a stochastic multi-objective method is used to manage the active and reactive power of EVs and harmonic compensation in smart distribution networks.

Hence, DERs and EVs are widely connected to the grid, which is inherently uncertain [8,9]. Uncertain parameters are the power production of DERs and the number and State Of Charge (SOC) of EVs which not considering them causes some problems in the study. Uncertainty modeling methods are different which include Information Gap-Decision Theory (IGDT) [10], robust optimization [11,12], fuzzy modeling [13,14], chance constraints [15], scenario-based methods [16], and Two-Point Estimation Method (2PEM) [17]. The increasing penetration rate of DERs and EVs in smart networks has emerged as problems in the field of grid voltage profiles. Any incorrect decision causes power quality problems. Therefore, the smart network scheduling problem associated with DERs, EVs, and their uncertainties to maintain appropriate voltage is much of interest. In this regard, many control methods are provided to solve the voltage problem and improve the network specifications. Different voltage control algorithms are developed based on centralized to distributed optimization methods [18-28]. The most basic method of voltage control is the centralized control method [18-20]. In a centralized control system, a central controller is used to control the voltage of the entire system in the presence of DERs. Disconnection with the central controller causes the voltage control system to lose in the entire system. In this method, there are a lot of computational burdens because the optimization is based on a lot of information. Also, since all system states and boundary conditions must be given to the central controller, this requires high-quality communication from all DERs to the central controller. There is a concern that the owners of various DERs are not willing to hand over their affairs to a third party due to

security. Therefore, centralized systems are usually not scalable and require many telecommunication links. In contrast, distributed control systems do not have a central controller, and the control system is distributed throughout the smart networks. In this structure, each DER is considered an independent control factor. Smart network components are related to each other on a Peer-to-Peer (P2P) basis in a distributed voltage control method. The distributed control methods can reach a globally optimal solution under certain constraints, thus achieving almost the same quality as centralized schemes.

There are different algorithms in the distributed voltage control method. The convergence speed of algorithms is important, and it is necessary to pay attention to it. The gossip algorithm is used in a distributed method to manage the power flows in the smart network. Each bus participates in distribution management by sending the calculated values to neighbor buses and using P2P communications [22]. In [23], voltage control is performed in a distributed method using the Dual-Decomposition (DD) algorithm. Also in this structure, P2P communication is used to exchange data between different parts of the network. In [24] a distributed feedback control algorithm is used to optimize the voltage. In this method, each bus can participate in voltage control by injecting active and reactive power. Each bus does this by measuring voltage and communicating with its neighbors. In [25], the problem is formulated based on the Alternating Direction Method of Multipliers (ADMM) algorithm and by dividing the network into specific regions. A two-stage method is used to optimize reactive power in distribution systems with Wind Farms (WFs). In this problem, border information is exchanged between neighboring regions. Also, In [26], the ADMM algorithm is used to control the active and reactive power of DERs of the type of WFs. According to this, WFs act in a way to minimize the deviation of bus voltage from the nominal value and network power losses. Also, the effects of active power injection from WFs are considered. The Jacobi Proximal-ADMM (JP-ADMM) algorithm is used based on distributed control method and P2P communication between smart photovoltaic inverters [27]. Also, in this control method, solutions are proposed to increase the robustness of the algorithm.

As mentioned, the use of EVs has expanded greatly. Therefore, the investigation of EVs and their control in distributed methods are also of great importance. In the mentioned papers in the field of distributed voltage

control, the presence of EVs is not reviewed in the smart distribution network. Also, the behavior of DERs and EVs is accompanied by uncertainties. Examining possible states is important to achieve more accurate results, but uncertainties are not included in most previous studies. In [28], the ADMM algorithm is used to solve the proposed model of decentralized robust optimization. In addition to DERs, EVs are also considered. The purpose of this issue is to achieve coordination between the aggregators of EVs and the Distribution Network Operator (DNO). In this model, EVs are under centralized control, and only DERs operate in a distributed manner. Therefore, this model is not fully distributed. It also seems that in this paper which models each EV independently, if the number of EVs is considered large, the optimization problem may not converge due to the use of many binary variables for modeling.

According to the research gaps mentioned in previous works, in this paper, distributed control methods are proposed based on DD and ADMM distributed algorithms using P2P communication capabilities of DER and EV converters considering the uncertainty related to DERs and EVs. These proposed algorithms use the change of active and reactive power of some DERs and the active discharge power of some EVs in the network to adjust the grid voltages.

Moreover:

- The considered EVs can discharge active power to the smart network in any parking lot. According to the voltage range, the algorithm determines how many of these EVs are allowed to be discharged for each hour, so the network does not suffer from overvoltage. It is assumed that the charging of EVs is done by the parking distributed generation sources to which the EV is connected, and they do not receive power for charging from the network.

- The uncertainty of solar radiation is also modeled using the scenario-based method per hour. Also, the uncertainty of the number of EVs in each parking lot and in each time slot is modeled using the 2PEM.

- For a better review, the results of the proposed algorithms are compared with the centralized control method.

- The effect of implementing proposed distributed algorithms is also investigated on grid losses in comparison to the centralized method.

2. General description of the proposed model

In this section, the smart network structure based on distributed voltage control is presented. Accordingly, Fig. 1 shows an overview of the proposed structure. In this model, day-ahead scheduling and one-hour time steps are considered. To achieve more accurate results, the uncertainty of solar radiation using the scenario-based method for each hour and the number of EVs in each parking lot using the 2PEM are modeled and applied to the smart active network. Smart photovoltaic inverters can help the power distribution system by using their decentralized voltage control feature. The proposed DD and ADMM algorithms are hosted by network voltage control functions and integrate with the smart photovoltaic inverter's internal control loops. In the physical layer, this network has n nodes, d smart photovoltaic inverters, and p distributed generation resource parking lots.
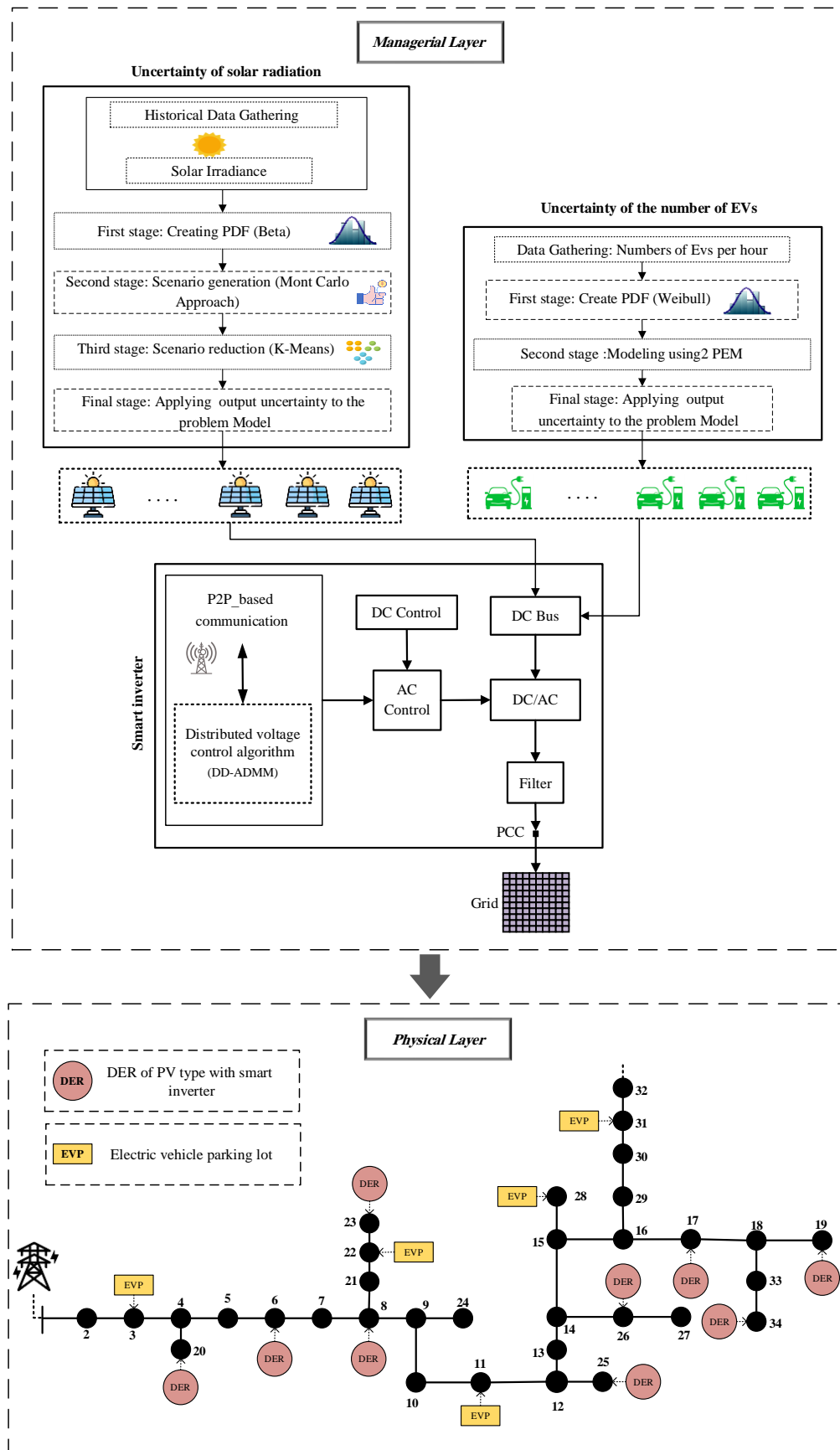
Fig. 1. *The proposed structure of a smart distribution network based on distributed voltage control.*

3. Mathematical model

In this section first, the mathematical model of the centralized voltage control problem is presented in subsection 3.1, since the aim is to find a method of converting the centralized optimization problem into a distributed optimization problem. On the other hand, by modeling the centralized voltage control problem, a basis can be obtained for comparison with the proposed distributed methods. In the following, the model of distributed algorithm based on DD and ADMM is presented in subsections 3.2 and 3.3, respectively.

3.1. Centralized control method

In this subsection, the problem model is introduced based on the centralized control method. The simplified model of the centralized control optimization problem is as follows:

$$min_{\Delta P, \Delta Q, \Delta P_p} \sum_d (c_d^P \Delta P_{d,t}^2 + c_d^Q \Delta Q_{d,t}^2) + \sum_p (c_p^P \Delta P_{p,t}^2) \tag{1}$$

$$\left| V_{n,t} \right| \leq V_{max}; \forall n, t \tag{2}$$

$$\left| V_{n,t} \right| \geq V_{min}; \forall n, t \tag{3}$$

$$\Delta P_{min,d} \leq \Delta P_{d,t} \leq \Delta P_{max,d}; \forall d, t \tag{4}$$

$$\Delta Q_{min,d} \leq \Delta Q_{d,t} \leq \Delta Q_{max,d}; \forall d, t \tag{5}$$

$$\Delta P_{min,p} \leq \Delta P_{p,t} \leq \Delta P_{max,p}; \forall p, t \tag{6}$$

The objective function (1) minimizes the amount of all changes in the active and reactive power of DERs required to maintain the voltage in the acceptable range, as well as the amount of change in the discharge of the active power of EVs in each hour. The first and second terms of this equation represent the change in active and reactive power of DERs with the value of $\Delta P_{d,t}$ and $\Delta Q_{d,t}$. Also, its third term shows the amount of change in the active discharge power of EVs. Constraints (2) and (3) indicate that the voltage value of each bus must be within the range. In the same way, the amount of change in active and reactive power of each DER in constraints (4) and (5) as well as the changes of active discharge power of EVs in constraint (6)

are limited. c_d^P, c_d^Q, and c_p^P are fixed penalty coefficients used to control variables of $\Delta P_{d,t}$, $\Delta Q_{d,t}$, and

$\Delta P_{p,t}$. These coefficients specify the priorities of the control measures. When the reactive power of DERs is

not enough or changing their active power is more optimal, the active power limit of DERs is used to adjust

the system voltage. To solve this optimization problem first, the voltage of each bus should be expressed as

a function of the active and reactive power of each DER and the active discharge power of each parking lot.

For simplicity, a simple two-bus distribution network is considered to consist of a DER, an Electric Vehicle

Parking lot (EVP), and a line with a resistance and a reactance as shown in Fig. 2.
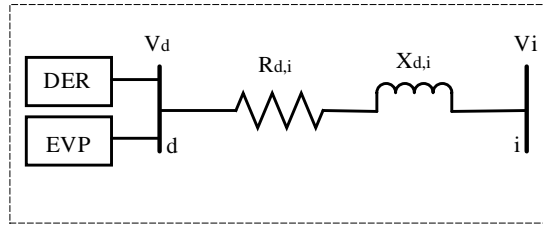
Fig. 2. *View of a simple distribution network in the presence of DERs and EVs.*

The voltage value of each bus can be obtained using equation (7):

$$\left| V_{i,t} \right| = \sqrt{(V_{d,t})^2 - 2(R_{d,i}P_{d,t} + X_{d,i}Q_{d,t} + R_{d,i}P_{p,t}) + \frac{(R_{d,i}^2 + X_{d,i}^2)(P_{d,t}^2 + Q_{d,t}^2 + P_{p,t}^2)}{(V_{d,t})^2}} \qquad (7)$$

Then, the active and reactive power of each DER and the amount of active discharge power of EVs can be

expressed as a function of their changes by (8), (9), and (10):

$$P_{d,t} = P_{d,0} + \Delta P_{d,t} \qquad (8)$$

$$Q_{d,t} = Q_{d,0} + \Delta Q_{d,t} \qquad (9)$$

$$P_{p,t} = P_{p,0} + \Delta P_{p,t} \qquad (10)$$

The operation of the centralized control method presented in this subsection is by using a central controller.

The central controller solves the optimization problem based on the information it receives about the voltage

of buses and the set points of DERs and EVs participating in the voltage control. The central controller sends

the new points $P_{d,t}$, $P_{p,t}$, and $Q_{d,t}$ to the desired DER and parking lot to adjust the voltage profile of the

distribution network. It should be noted that the equations mentioned are developed based on the method presented in [27].

3.2. Proposed DD-based distributed control

The main aim of this paper is to design a voltage control system that does not rely on a central controller. In this subsection, the distributed voltage control algorithm is proposed based on the DD method [23]. This proposed algorithm decomposes the optimization problem into subproblems suitable for distributed control and applies the Lagrangian theory. To do this, the centralized optimization problem (1)-(6) should be decomposed into optimization subproblems so that they can be solved locally. The objective function (1) can be solved in distributed form. Also, constraints (4), (5), and (6) are local, meaning they only influence the local decision variables of $\Delta P_{d,t}$, $\Delta Q_{d,t}$, and $\Delta P_{p,t}$. Therefore, these constraints can be easily separated into local constraints. On the other hand, constraints (2) and (3) cannot be distributed because the voltage of each bus is a non-linear function of $P_{d,t}$, $Q_{d,t}$, and $P_{p,t}$ given by equation (7) is described. By linearizing the voltage of each bus, the optimization problem (1)-(6) is solved using the proposed DD-based method. The first-order approximation of equation (7) can be used to linearize the voltage of each bus, as described in equation (11).

$$\left|V_{n,t}\right| \approx V_{n,0} + \sum_{d}\left(\frac{\partial\left|V_{n,t}\right|}{\partial P_{d,t}}\Delta P_{d,t} + \frac{\partial\left|V_{n,t}\right|}{\partial Q_{d,t}}\Delta Q_{d,t}\right) + \sum_{p}\left(\frac{\partial\left|V_{n,t}\right|}{\partial P_{p,t}}\Delta P_{p,t}\right) \tag{11}$$

Therefore, according to equation (11), $\left|V_{n,t}\right|$ is separated with sensitivity to active and reactive power. In the following, since the calculation of partial derivatives is not easy and depends on the state of the system, they can be approximated using equations (12), (13), and (14).

$$\frac{\partial\left|V_{n,t}\right|}{\partial P_{d,t}} \cong \frac{R_{d,i}}{V_{nom}} \tag{12}$$

$$\frac{\partial\left|V_{n,t}\right|}{\partial Q_{d,t}} \cong \frac{X_{d,i}}{V_{nom}} \tag{13}$$

$$\frac{\partial \left| V_{n,t} \right|}{\partial P_{p,t}} \cong \frac{R_{d,i}}{V_{nom}} \tag{14}$$

The above equations are a suitable approximation for $\left| V_{n,t} \right|$ when the phase angle between voltages in different buses is small, which can be proven in the distribution network. The linearization $\left| V_{n,t} \right|$ provides the possibility of solving the entire optimization problem (1)-(6) in a distributed method based on the Lagrangian DD method. The main idea of the Lagrangian method is to simplify the original problem (1)-(6) by transferring the constraints to the objective function. The Lagrange of the objective function (1) is defined as follows:

$$L(\Delta P, \Delta Q, \Delta P_p, \lambda^{max}, \lambda^{min}) = \sum_d (c_d^P \Delta P_{d,t}^2 + c_d^Q \Delta Q_{d,t}^2)$$
$$+ \sum_p (c_p^P \Delta P_{p,t}^2) + \sum_n \lambda_{n,t}^{max} (\left| V_{n,t} \right| - V_{max}) + \lambda_{n,t}^{min} (V_{min} - \left| V_{n,t} \right|) \tag{15}$$

Where $\lambda_{n,t}^{max}$ and $\lambda_{n,t}^{min}$ are the Lagrangian multipliers, which are associated with inequality constraints (2) and (3), respectively. Based on (11), equation (15) can be written as follows:

$$L = \sum_d (c_d^P \Delta P_{d,t}^2 + c_d^Q \Delta Q_{d,t}^2) + \sum_p (c_p^P \Delta P_{p,t}^2) + \tag{16}$$
$$\sum_n \lambda_{n,t}^{max} (V_{n,0} - V_{max} + \frac{R_{d,i}}{V_{nom}} \Delta P_{d,t} + \frac{X_{d,i}}{V_{nom}} \Delta Q_{d,t} + \frac{R_{d,i}}{V_{nom}} \Delta P_{p,t})$$
$$+ \lambda_{n,t}^{min} (V_{min} - V_{n,0} - \frac{R_{d,i}}{V_{nom}} \Delta P_{d,t} - \frac{X_{d,i}}{V_{nom}} \Delta Q_{d,t} - \frac{R_{d,i}}{V_{nom}} \Delta P_{p,t})$$

In (16), if the value of the Lagrange multipliers is considered constant, the previous objective function can be considered for each of the smart inverters connected to DERs and for each parking lot with EVs individually. To solve equation (16) more easily, the minimum value of the objective function can be obtained using partial derivatives and the Karush-Kuhn–Tucker conditions (KKT) with equations (17), (18), and (19) as follows:

$$\Delta P_{d,t}(\lambda^{max}, \lambda^{min}) = \frac{1}{2c_d^P} \sum_n \left(\lambda_{n,t}^{min} - \lambda_{n,t}^{max} \right) \frac{R_{d,i}}{V_{nom}} \tag{17}$$

$$\Delta Q_{d,t}(\lambda^{max},\lambda^{min}) = \frac{1}{2c_d^Q}\sum_n\left(\lambda_{n,t}^{min}-\lambda_{n,t}^{max}\right)\frac{X_{d,i}}{V_{nom}} \tag{18}$$

$$\Delta P_{p,t}(\lambda^{max},\lambda^{min}) = \frac{1}{2c_p^P}\sum_n\left(\lambda_{n,t}^{min}-\lambda_{n,t}^{max}\right)\frac{R_{d,i}}{V_{nom}} \tag{19}$$

Lagrangian multipliers must be greater than zero. According to KKT rules, Lagrange multipliers are obtained from equations (20) and (21):

$$\lambda_{n,t}^{max,k} = max\left\{\lambda_{n,t}^{max,k-1}+\alpha\left(V_{max}-\left|V_{n,t}\right|\right),0\right\} \tag{20}$$

$$\lambda_{n,t}^{min,k} = max\left\{\lambda_{n,t}^{min,k-1}+\alpha\left(\left|V_{n,t}\right|-V_{min}\right),0\right\} \tag{21}$$

Where k is the number of iterations and α is a parameter that is defined to accelerate the convergence of the algorithm. Since the Lagrangian multipliers have a direct relationship with the voltage difference of a bus from the network, it seems logical that each pair of Lagrangian multipliers is calculated locally in the bus to which it belongs. From P2P communication protocols are used to obtain $\lambda_{n,t}^{max}$ and $\lambda_{n,t}^{min}$. Since the proposed algorithm in this subsection does not have a suitable convergence speed, the ADMM-based algorithm is proposed in the next section.

3.3. ADMM-based distributed control

In this subsection first, the formulation of the ADMM algorithm is described in general in part 3.3.1. Then the details of the formulation of the proposed ADMM-based algorithm are reviewed in part 3.3.2.

3.3.1. ADMM method

The ADMM algorithm used for optimization problems can be written as follows [29]:

$$Min(f(x)+g(z)), x\in X, z\in Z \tag{22}$$

$$Ax+Bz=c \tag{23}$$

Constraint (23) can be added to the objective function. Therefore, the Lagrange of the objective function is obtained as follows:

$$MinL_\rho(x,z,\lambda) = f(x) + g(z) + \lambda^T(Ax + Bz - c) + \frac{\rho}{2}\|Ax + Bz - c\|_2^2, x \in X, z \in Z \tag{24}$$

In this equation, λ represents the Lagrangian multiplier, and ρ is a penalty factor related to the constraint (23), which should be considered positive, and $\|.\|2$ is the norm of a vector. The Lagrangian function obtained in (24) can be solved by the ADMM algorithm using the iteration of equations (25)-(27). In these equations, k is the iteration index of the algorithm. In this algorithm, the variables x and z are optimized according to equations (25) and (26), respectively. Thus, the ADMM algorithm becomes an effective method to optimize the problem.

$$x(k+1) = \arg\min L_\rho(x, z(k), \lambda(k)), x \in X \tag{25}$$

$$z(k+1) = \arg\min L_\rho(x(k+1), z, \lambda(k)), z \in Z \tag{26}$$

$$\lambda(k+1) = \lambda(k) + \rho(Ax(k+1) + Bz(k+1) - c) \tag{27}$$

Finally, the ADMM algorithm converges when the following equation holds:

$$\|\lambda(k+1) - \lambda(k)\|_2 \le \varepsilon_{thr} \tag{28}$$

3.3.2. Proposed ADMM-based algorithm

This part details the ADMM-based proposed distributed algorithm formulation for this special problem. The ADMM-based algorithm also applies terms called penalty coefficients to the Lagrange function. This algorithm, like the DD-based algorithm, is used to decompose a voltage control system based on centralized optimization into subsystems that interact with each other in a distributed manner. By transferring the global constraints to the objective function, the Lagrange of the objective function is defined as equation (29):

$$L_\rho(\Delta P, \Delta Q, \Delta P_p, \lambda^{max}, \lambda^{min}) = \sum_d (c_d^P \Delta P_{d,t}^2 + c_d^Q \Delta Q_{d,t}^2) + \sum_p (c_p^P \Delta P_{p,t}^2) + \tag{29}$$

$$\sum_n \lambda_{n,t}^{max}(|V_{n,t}| - V_{max}) + \lambda_{n,t}^{min}(V_{min} - |V_{n,t}|) + \frac{\rho}{2}\||V_{n,t}| - V_{max}\|_2^2 + \frac{\rho}{2}\|V_{min} - |V_{n,t}|\|_2^2$$

Like the proposed DD-based algorithm, $\lambda_{n,t}^{max}$ and $\lambda_{n,t}^{min}$ are the Lagrangian multipliers, which are associated with unequal constraints (2) and (3), respectively. According to KKT rules, Lagrangian multipliers are obtained from equations (30) and (31):

$$\lambda_{n,t}^{max,k} = max \left\{ \lambda_{n,t}^{max,k-1} + \rho\left(V_{max} - \left|V_{n,t}\right|\right), 0 \right\} \tag{30}$$

$$\lambda_{n,t}^{min,k} = max \left\{ \lambda_{n,t}^{min,k-1} + \rho\left(\left|V_{n,t}\right| - V_{min}\right), 0 \right\} \tag{31}$$

To solve equation (29) more easily, using partial derivatives and KKT rules, the minimum value of the objective function can be obtained with equations (32), (33), and (34):

$$\Delta P_{d,t} = \frac{1}{2c_d^P + 2\rho\left(\dfrac{R_{d,i}}{V_{nom}}\right)^2} \left[-2\rho\left(\frac{R_{d,i}}{V_{nom}}\right)^2 \Delta P_{p,t} - 2\rho\frac{R_{d,i}X_{d,i}}{V_{nom}^2}\Delta Q_{d,t} + A_t^R \right] \tag{32}$$

$$\Delta Q_{d,t} = \frac{1}{2c_d^Q + 2\rho\left(\dfrac{X_{d,i}}{V_{nom}}\right)^2} \left[-2\rho\frac{R_{d,i}X_{d,i}}{V_{nom}^2}\left(\Delta P_{d,t} + \Delta P_{p,t}\right) + A_t^X \right] \tag{33}$$

$$\Delta P_{p,t} = \frac{1}{2c_p^P + 2\rho\left(\dfrac{R_{d,i}}{V_{nom}}\right)^2} \left[-2\rho\left(\frac{R_{d,i}}{V_{nom}}\right)^2 \Delta P_{d,t} - 2\rho\frac{R_{d,i}X_{d,i}}{V_{nom}^2}\Delta Q_{d,t} + A_t^R \right] \tag{34}$$

In the above equations, the values of A_t^R and A_t^X obtain using equations (35)-(38). From P2P communication protocols are used to achieve $\lambda_{n,t}^{max}$ and $\lambda_{n,t}^{min}$ of all buses.

$$A_t^R = \sum_n a_{n,t}^R \tag{35}$$

$$A_t^X = \sum_n a_{n,t}^X \tag{36}$$

$$a_{n,t}^R = \left(\lambda_{n,t}^{min} - \lambda_{n,t}^{max}\right)\frac{R_{d,i}}{V_{nom}} \tag{37}$$

$$a_{n,t}^{X} = \left(\lambda_{n,t}^{min} - \lambda_{n,t}^{max} \right) \frac{X_{d,i}}{V_{nom}} \tag{38}$$

Fig. 3 shows the flowchart of problem-solving using the proposed ADMM-based algorithm. In the following, the Voltage Deviation Index (VDI) and the Average Voltage Deviation Index (AVDI) are introduced in equations (39) and (40), respectively. By using these two indices can be seen the effect of the proposed methods, and can also be used as a basis for comparing all methods.

$$\left(VDI \right)_{n} = \sum_{t} \left(\left| V_{n,t} \right| - 1 \right)^{2} \tag{39}$$

$$AVDI = \left(\sum_{n} \sum_{t} \left(\left| V_{n,t} \right| - 1 \right)^{2} \right) / N \tag{40}$$
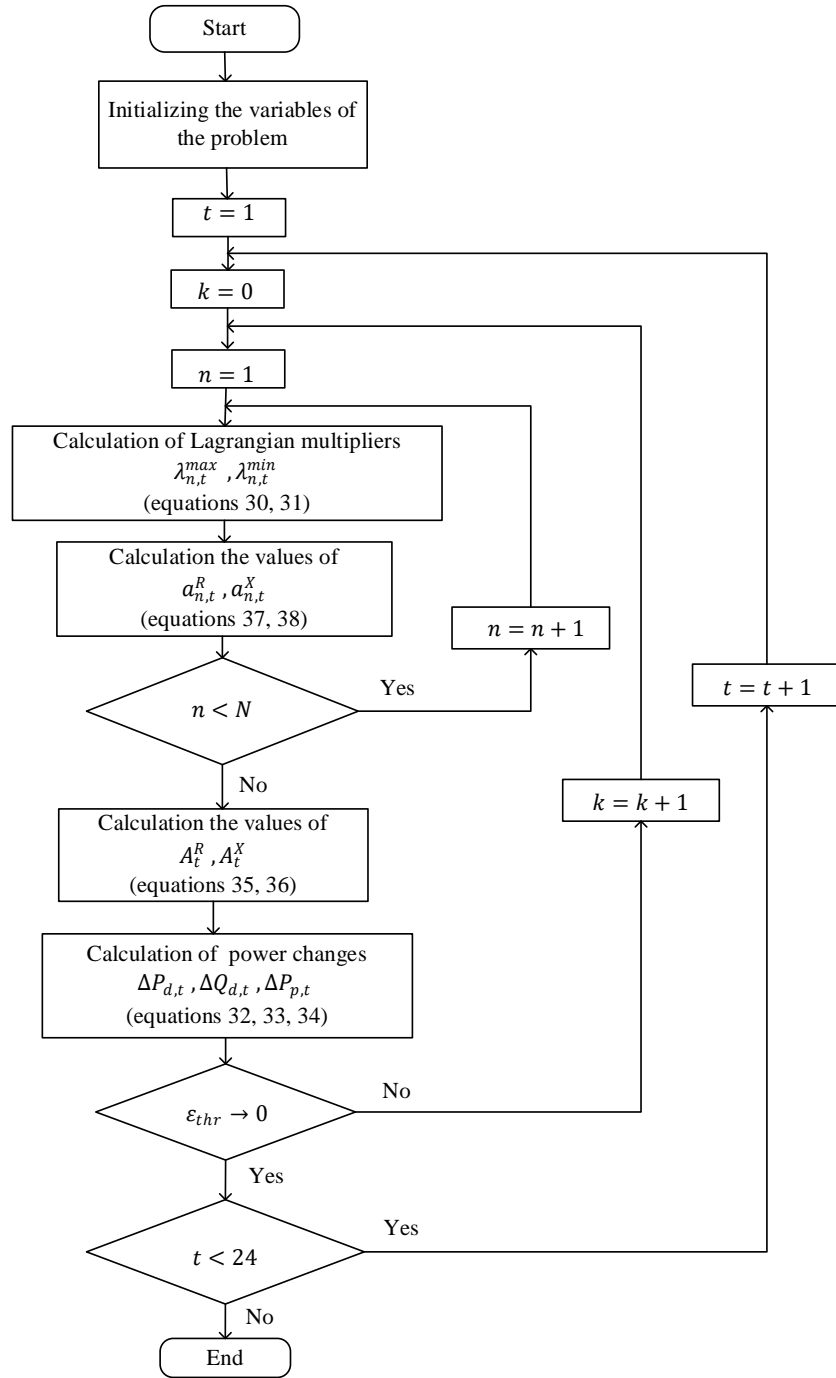
Fig. 3. *Flowchart of the proposed ADMM algorithm.*

3.4. Network losses

In a power system, part of the available power is lost by unwanted effects. During the transmission of electric power, there are also losses due to the resistance and reactance of the line. In this paper, the effect of the proposed methods on network losses is also investigated. The amount of line active power losses between two buses n and j can be obtained by equation (41).

$$P_{Loss}(n,j) = R_{n,j} \frac{\left(P_{n,j}^2 + Q_{n,j}^2\right)}{\left|V_n\right|^2} \qquad (41)$$

The total active power losses of the network can be determined by the sum of the losses of all lines, which is expressed as equation (42).

$$P_{(n,j)}^{T,Loss} = \sum_L P_{(n,j)}^{Loss} \quad \forall n,j \in L \qquad (42)$$

3.5. Uncertainty model

In this subsection, the mathematical formulation of the uncertainties used in this paper is investigated.

3.5.1. Uncertainty of solar radiation

Among the different methods of uncertainty modeling, the scenario-based method is used for uncertainty modeling of solar radiation.

In this modeling method:

- Step 1: Using the collected data, a Probability Distribution Function (PDF) is produced, and also at this stage, choosing the type of PDF is very important. The uncertainty of the amount of solar radiation is usually modeled by the beta distribution function, which is expressed by equations (43) and (44) [30].

$$f(x:\alpha,\beta) = \frac{\gamma(\alpha+\beta)}{\gamma(\alpha)\gamma(\beta)} x^{\alpha-1}(1-x)^{\beta-1} \qquad (43)$$

$$\gamma(n) = (n-1)! \qquad (44)$$

- Step 2: In this step, using the Monte Carlo approach, scenarios are generated and the number of these scenarios is large for modeling.

- Step 3: In this step, the scenarios can be reduced by using different methods such as Mixed Integer Linear Programming (MILP), fuzzy, and K-Means clustering. In this modeling, the K-Means method is used to reduce the scenarios.

In this method, it is assumed that the set $\{x_1, x_2, \ldots, x_n\}$ is all the scenarios produced in the previous step and each scenario is a d-dimensional vector. K-Means clustering aims to divide n scenarios into k clusters or segments in which k sections are specified as a set $s = \{s_1, s_2, \ldots, s_k\}$. The members of this set should be chosen in such a way as to minimize the Within-Cluster Sum of Squares (WCSS) according to equation (45) [31].

$$argmin_s \sum_{i=1}^{k} \sum_{x \in s_i} \|x - \mu_i\|^2 = argmin_s \sum_{i=1}^{k} |s_i| Vars_i \tag{45}$$

In (45), μ_i is the mean of the points in each cluster or in other words in each s_i, and $|s_i|$ is the number of cluster members i.

- Final step: In this step, the Expected value of the scenarios obtained in the previous step is calculated and finally, the modeled uncertainty is applied to the problem models.

3.5.2. EVs participation uncertainty

Also in this paper, the number of EVs in each parking lot and in each time slot is modeled by the 2PEM. For this purpose, using the Weibull distribution function, the collected data are modeled. The Weibull distribution function is defined by shape and scale parameters, which is expressed by equation (46) [32].

$$f(x : \lambda, k) = \frac{k}{\lambda} \left(\frac{x}{\lambda}\right)^{k-1} e^{-\left(\frac{x}{\lambda}\right)^k} \quad, \quad x \geq 0 \tag{46}$$

In the above equation, k is the shape parameter and λ is the scale parameter. After modeling the data by the Weibull distribution function, 2PEM is used to model the mentioned uncertainty [33]. For this probabilistic modeling, it is assumed that in the function $z = h(x)$, x is a vector as $\{x_1, x_2, \ldots, x_m\}$ which x_1 to x_m are random parameters modeled by the PDF. h describes the system model, x is the vector of uncertain input parameters to the system, and finally, z is the output variable. In this modeling method, the position of the estimated points of the x is obtained using equation (47).

$$x_i = \mu_x + \epsilon_i \times \delta_x \qquad i = 1, 2 \tag{47}$$

Here, since the number of estimated points is two, $i = 1, 2$ is assumed, and x_i is the focus position i. The required parameters are calculated by equations (48), (49), and (50).

$$\epsilon_i = \frac{\lambda_{x,3}}{2} + (-1)^{3-j} \sqrt{1 + \left(\frac{\lambda_{x,3}}{2}\right)^2} \qquad j = 1, 2 \tag{48}$$

$$M_j(x) = \int_{-\infty}^{+\infty} (x - \mu_x)^j f_x(x) dx \tag{49}$$

$$\lambda_{x,j} = \frac{M_j(x)}{\delta_x^{\ j}} \qquad j = 1, 2, 3, \dots \tag{50}$$

$M_j(x)$ specifies the central torque of order j of variable x, also μ_x and δ_x represent the mean and standard deviation, respectively. The probability of each part is calculated by equations (51) and (52).

$$P_j = \frac{(-1)^j \epsilon_{3-j}}{\epsilon} \tag{51}$$

$$\epsilon = \epsilon_1 - \epsilon_2 = 2\sqrt{1 + \left(\frac{\lambda_{x,3}}{2}\right)^2} \tag{52}$$

The torque of random quantity z is calculated with appropriate approximation by equation (53).

$$E(z^j) = \sum_{i=1}^{2} P_i (h(x_i))^j \tag{53}$$

Finally, this calculated uncertainty is applied to the structure of the problem, such as the uncertainty of solar radiation.

4. Numerical analysis

In this section first, the information on the network is given in subsection 4.1, and then the obtained results are presented in subsection 4.2.

4.1. System data

To check the performance of the proposed algorithms, the modified IEEE 69-bus radial distribution network is selected as the test system, and simulation is performed on this network [34]. Fig. 4 shows the overview of the network considering DERs and EVPs, and the network load profile is considered in Fig. 5. The minimum and maximum voltage limits are set at 0.95 and 1.05 p.u. The values of rated voltage and rated power are considered to be 12.66 kV and 10 MVA, respectively. In this paper, the problem of voltage control is solved in a centralized method, and distributed method based on DD and ADMM proposed algorithms by GAMS software. The reviewed uncertainties are also modeled by MATLAB software, and the obtained results are entered into GAMS software. All modeling methods are performed using a computer system with 4 GB of RAM and an inter-core i5 CPU.
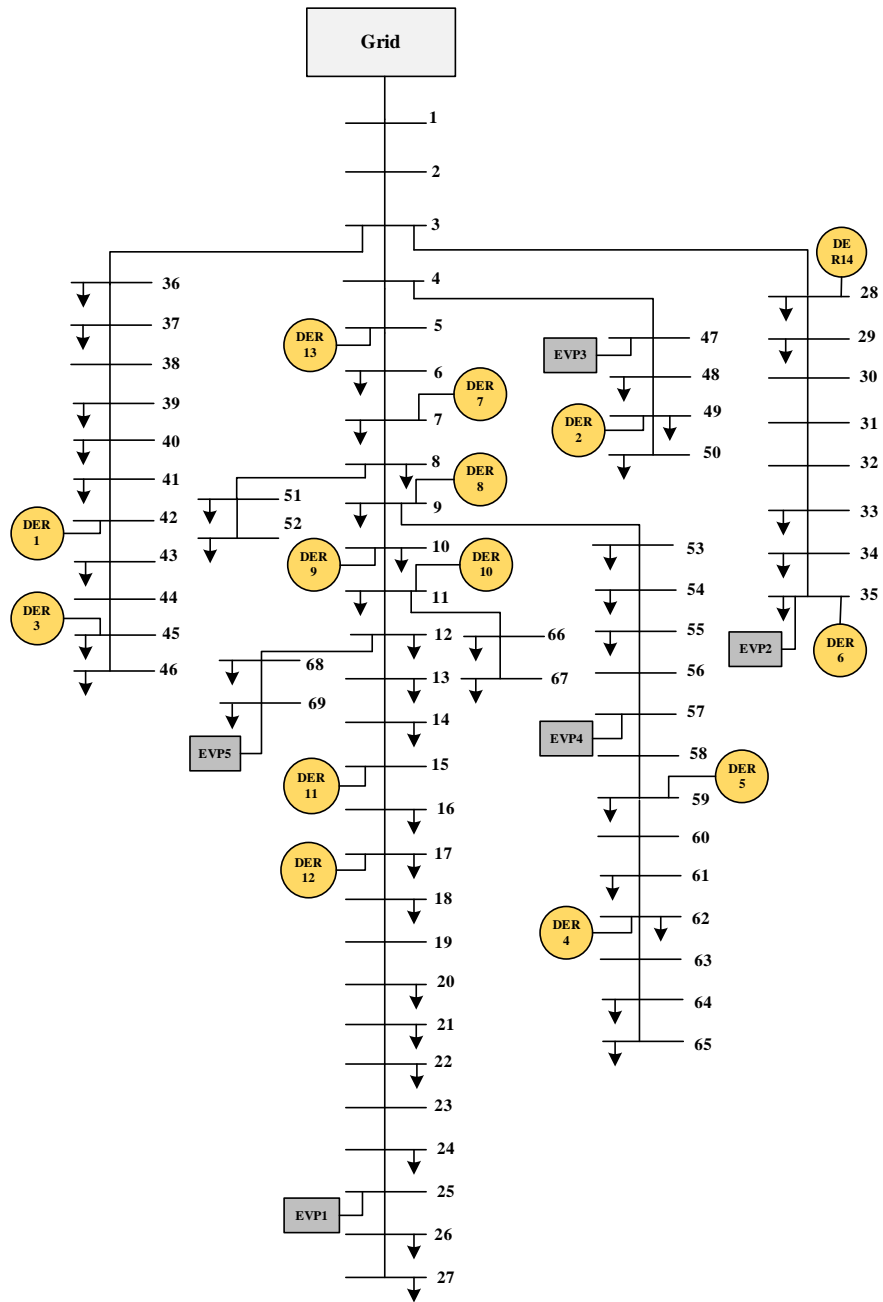
Fig. 4. *IEEE 69-bus radial distribution system.*
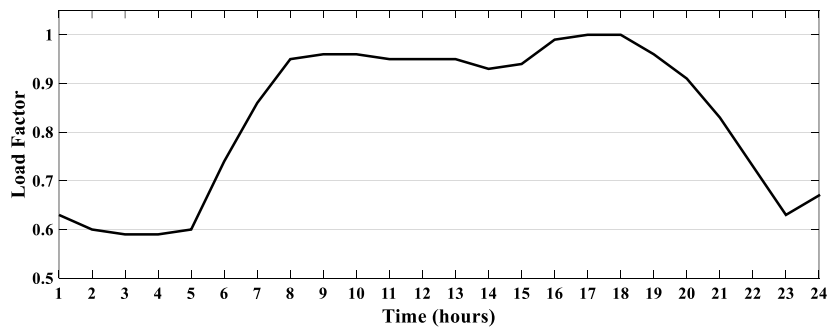
Fig. 5. *The network load profile.*

The fourteen solar-type DERs are considered in the discussed radial network. It is also important to note that the location of DERs along this feeder is hypothetical. It is assumed that each DER has a three-phase smart photovoltaic inverter, and all these inverters participate in voltage control. Each inverter has network management functions that allow it to adjust the voltage at the Point of Common Connection (PCC).

This network also has five EVPs, and the placement of these EVPs like DERs is completely hypothetical. As mentioned, these EVs can discharge active power to the network, and their charging is provided by the parking lot itself. Algorithms determine the number of EVs that can be discharged per hour. The rest of the EVs can discharge there if needed by considering the storage device inside the parking lots. α and ρ are set to 20 and 0.08, respectively. c_d^P, c_d^Q, and c_p^P values are also set to 4, 1, and 2, respectively.

4.2. Study results

In this subsection, the results are presented and compared with each other. According to Table 1, the results are examined in five scenarios.

Table 1 Different scenarios in the case study.

Scenario number	Centralized control method	DD-based distributed algorithm	ADMM-based distributed algorithm	Presence of DER	Presence of EV
1	✓			✓	
2		✓		✓	
3			✓	✓	
4		✓		✓	✓
5			✓	✓	✓

4.2.1. Scenario 1 (Centralized control method)

The centralized voltage control method is investigated, in this scenario. In this regard, Fig. 6 and Fig. 7 show bus voltage 61 and 65 in the base case without DER and centralized voltage control method, respectively. Bus 61 has the highest amount of load, and bus 65 has the highest VDI. For this reason, these two buses are used for the case study. As can be seen from the figures, no voltage improvement is done since 21-4. Because during these hours the DERs have no production, and the network is without these resources. It is expected that the voltage improvement in the centralized method is more than in the proposed distributed methods, which are investigated in the next two scenarios. The total grid losses are approximately 0.2806 p.u in the

base case without DERs, and it has reached 0.1675 p.u in the centralized control method. Therefore, by improving the voltage, network losses will also decrease.
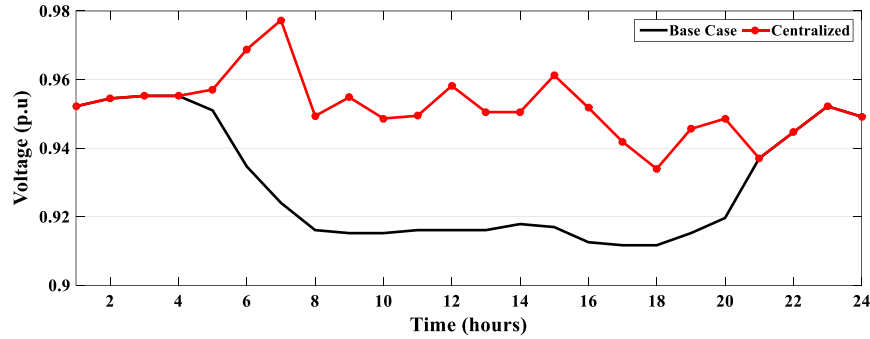

Fig. 6. *61 bus voltage curve.*
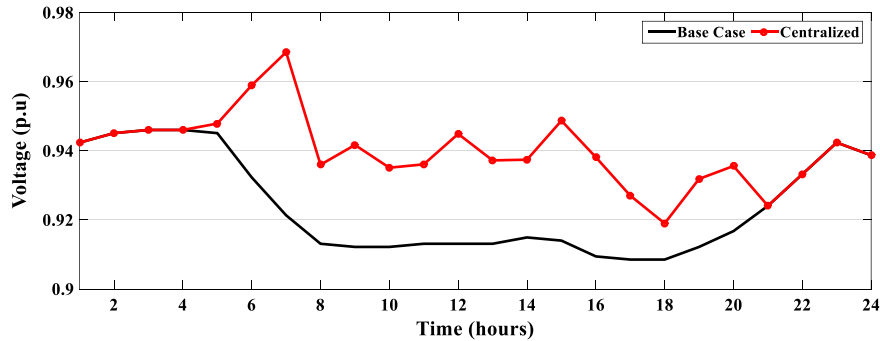
Fig. 7. *65 bus voltage curve.*

4.2.2.   Scenario 2 (DD-based distributed algorithm)

In this scenario, the aim is to investigate the distributed voltage control method based on the DD algorithm. Fig. 8 and Fig. 9 show the voltage of buses 61 and 65, respectively. For a better comparison, the results of this control method are drawn together with the centralized control method. As expected, the voltage control by the centralized method is performed better in all hours than the DD-based distributed method, but due to the mentioned advantages, this control method is suggested. However, due to the slow convergence speed and the low required power to improve the voltage, which will be examined below, this method is not very efficient. For this reason, ADMM-based distributed control is proposed in the next scenario.
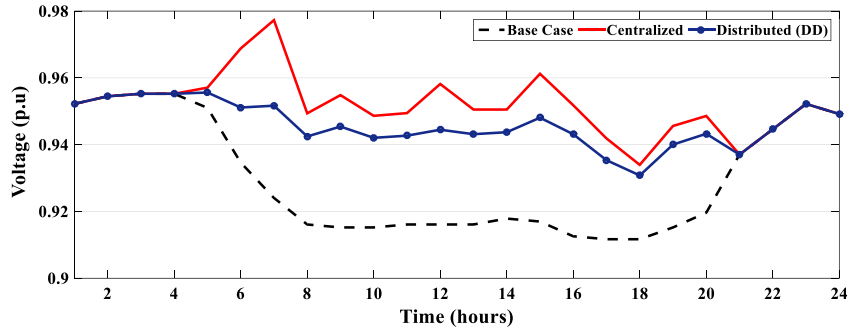
Fig. 8. *61 bus voltage curve.*
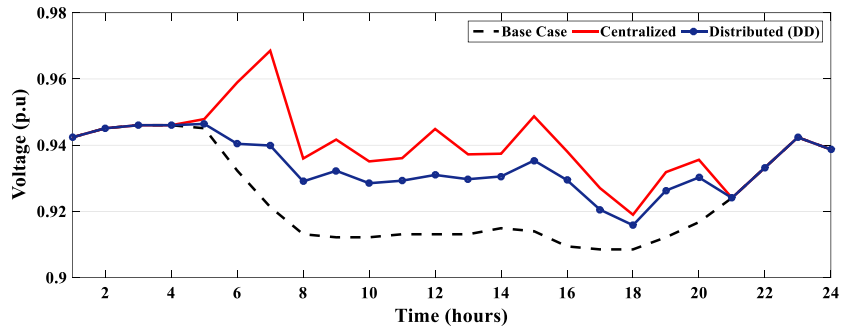
Fig. 9. *65 bus voltage curve.*

4.2.3. *Scenario 3 (ADMM-based distributed algorithm)*

Considering the disadvantages mentioned in the proposed DD-based method, the ADMM-based distributed control method is proposed, in this scenario. For this purpose, Fig. 10 and Fig. 11 show the voltage of buses 61 and 65 as in the previous scenarios, respectively. As can be seen from the figures, for both buses, the proposed ADMM-based algorithm performed better than the DD-based algorithm, and it has results closer to the centralized control method.
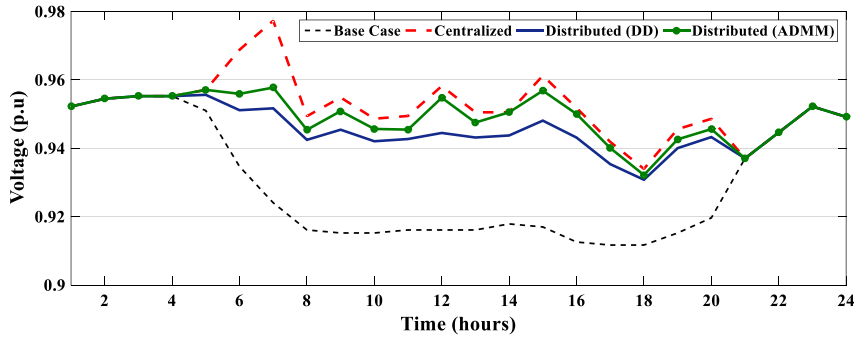
Fig. 10. *61 bus voltage curve.*
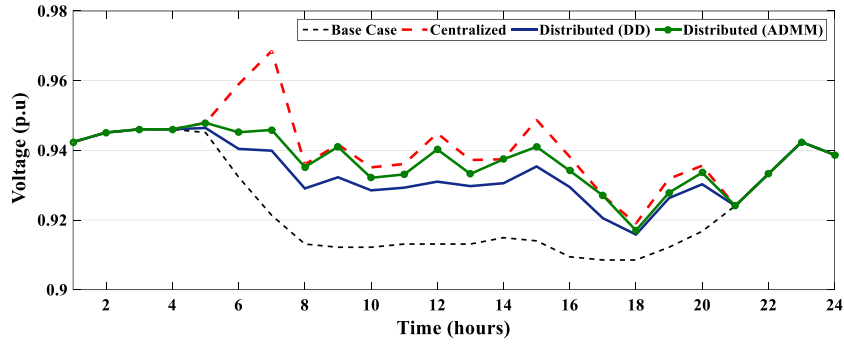
Fig. 11. *65 bus voltage curve.*

Fig. 12 shows the Lagrangian multiplier of DER4, which is connected to bus 62. As can be seen, it starts to adjust the voltage from 4:00 and reaches its maximum value at 18:00. Fig. 13 shows the active and reactive power changes of the DER4 smart inverter in bus 62. The total active power supplied to the network by this source during the day is about 0.1841 p.u, and the total reactive power is about 0.1564 p.u.
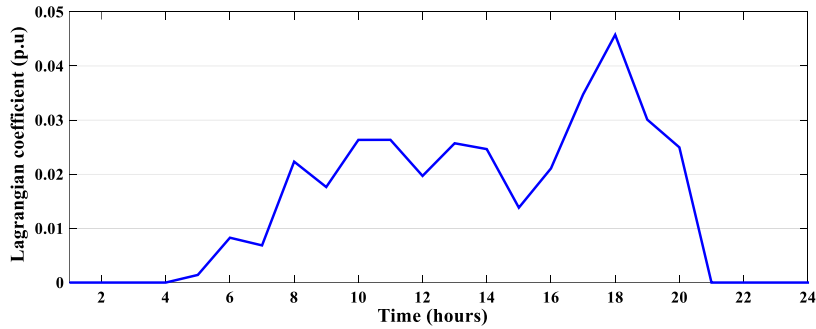

**Fig. 12.** *DER4 Lagrangian multiplier curve.*
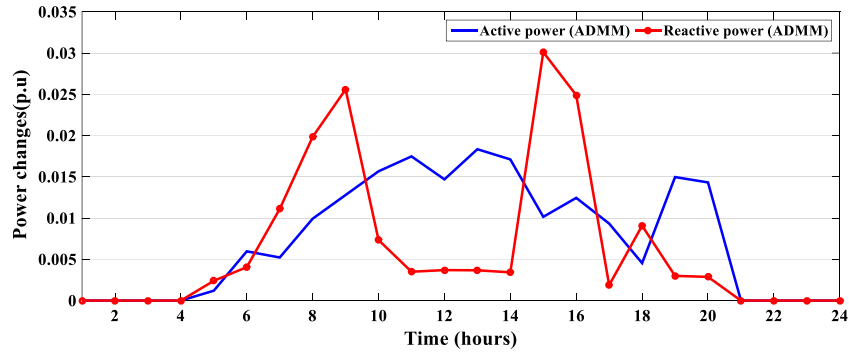
Fig. 13. *DER4 active and reactive power changes curve.*

In the following, to show the disadvantages of the proposed DD-based algorithm, it is compared with the proposed ADMM-based algorithm without the presence of EVs. For this purpose, Fig. 14 and Fig. 15 show the amount of active and reactive power changes of the smart inverter of DER4 at 11:00, and Fig. 16 shows the voltage of bus 61 at 16:00.
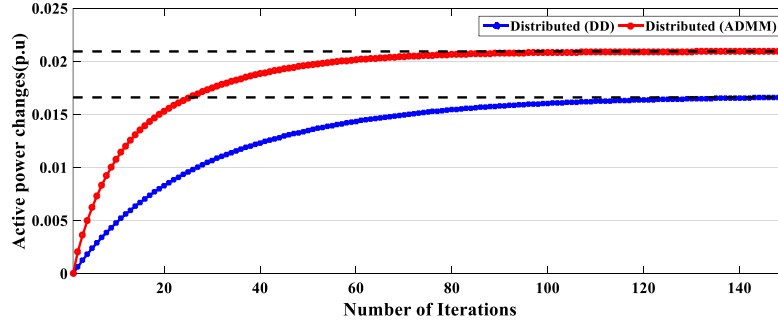

**Fig. 14.** *Active power change curve of DER4 at 11:00.*
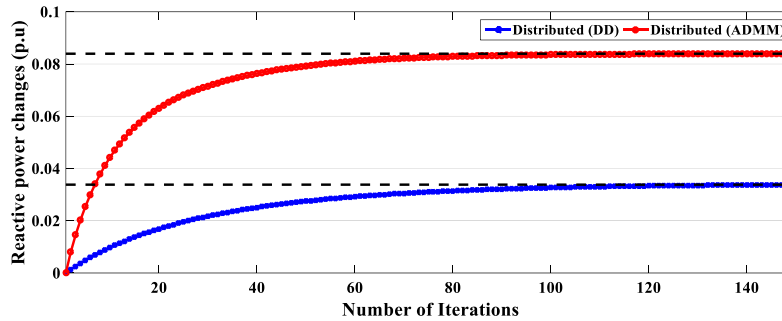
Fig. 15. *Reactive power change curve of DER4 at 11:00.*
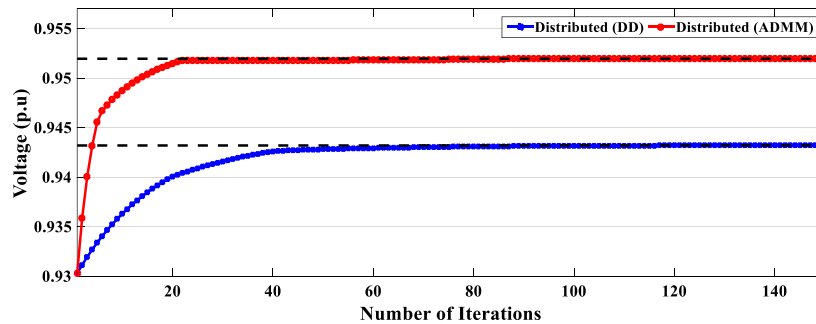

Fig. 16. *61 bus voltage curve at 16:00.*

According to Fig. 14 and Fig. 15, the ADMM-based algorithm has a higher convergence speed than the DD-based algorithm, and convergence is achieved about 20 iterations earlier. Fig .16 shows the advantage of the proposed ADMM-based algorithm in the voltage curve like the active and reactive power changes. In such a

way the bus voltage is increased from 0.93 to approximately 0.952, while the DD-based algorithm is

increased the voltage from 0.93 to approximately 0.943. Also, the higher convergence speed of the ADMM-

based algorithm can be better seen in this curve. Fig. 17 shows the comparison of total network losses in 24

hours for all methods. It should be noted that the base case without DER and the centralized control method

are without iteration, but in this figure, they are drawn as a line to better see the results.
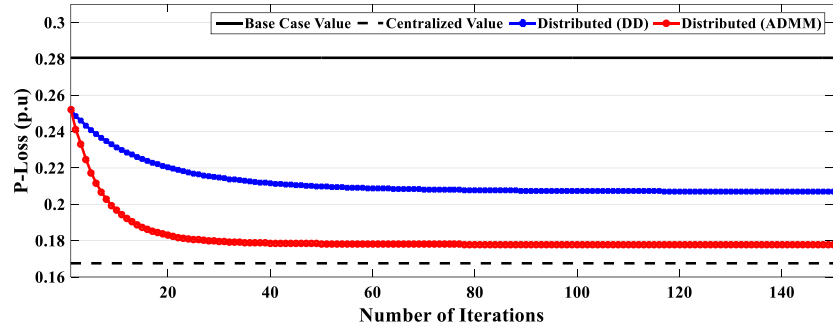
Fig. 17. *Total grid losses in 24 hours.*

As expected, by the improvement of voltage, the centralized control method has power losses lower than

the proposed distributed methods. In the comparison of distributed methods, the proposed ADMM-based

algorithm has reduced the losses more than the proposed DD-based algorithm.

4.2.4. *Scenario 4 (DD-based algorithm with EV)*

In this scenario, the effect of the presence of EVs in the network is investigated by implementing the proposed

DD-based algorithm. Fig. 18 shows the voltage curve of bus 61 for the DD-based algorithm. As can be seen,

in the presence of EVs, voltage improvement is done better.
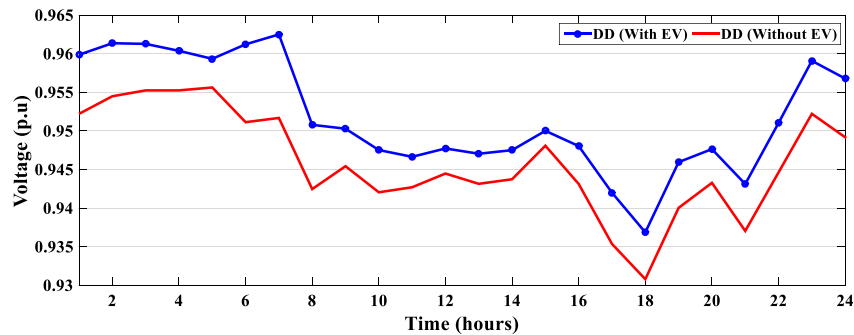
Fig. 18. *61 bus voltage curve by implementing the DD algorithm.*

Fig. 19 shows the power losses curve of the entire network in two modes. In this figure, the losses are decreased more in the presence of EVs, and this is because the voltage improvement is done better in the presence of EVs.
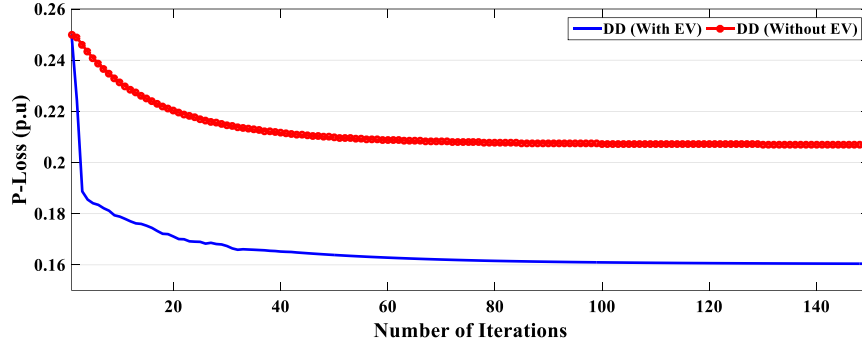

Fig. 19. *Total losses curve in 24 hours by implementing the DD algorithm.*

4.2.5. *Scenario 5 (ADMM-based algorithm with EV)*

In this scenario, the effect of the presence of EVs in the network is investigated by implementing the proposed ADMM-based algorithm. The presence of EVs in the ADMM-based algorithm, like the DD-based algorithm, improves voltage and reduces grid losses. For this purpose, Fig. 20 and Fig. 21 show the comparison of bus 61 voltage and total grid losses in the presence and absence of EVs, respectively.
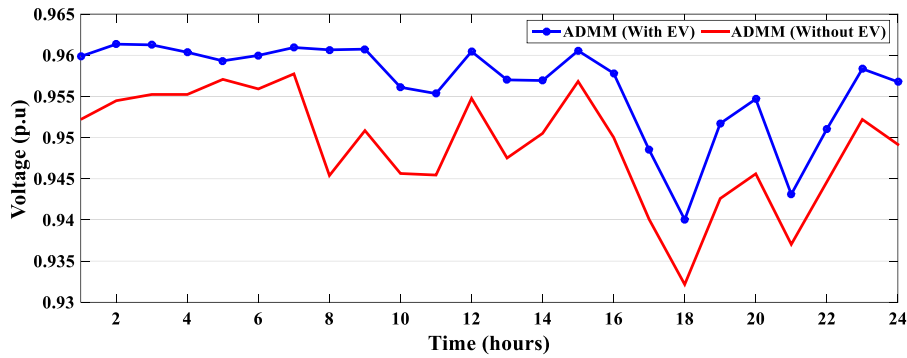

**Fig. 20.** *61 bus voltage curve by implementing the ADMM algorithm.*
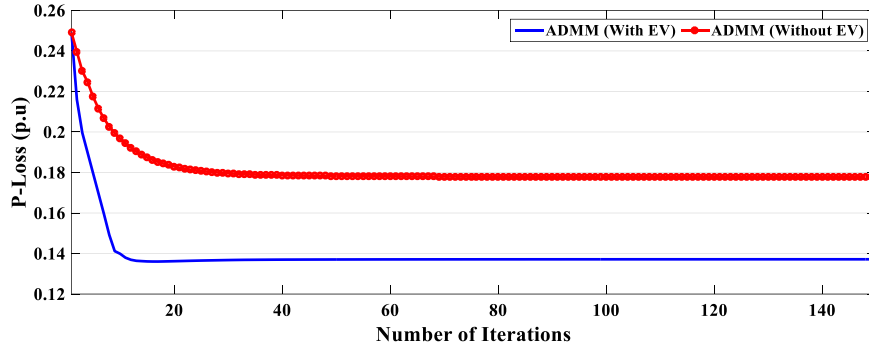
Fig. 21. *Total losses curve in 24 hours by implementing the ADMM algorithm.*

4.2.6. *Comparison of probabilistic and deterministic modes*

In this subsection, the comparison of probabilistic and deterministic modes is discussed. It should be noted that all the previous scenarios were probabilities, and the uncertainty is included related to the amount of solar radiation and the number of EVs in each parking lot in all of them. Fig. 22 and Fig. 23 show the voltage of buses 61 and 65, respectively. As expected, the results are better in the case of not considering the uncertainty.
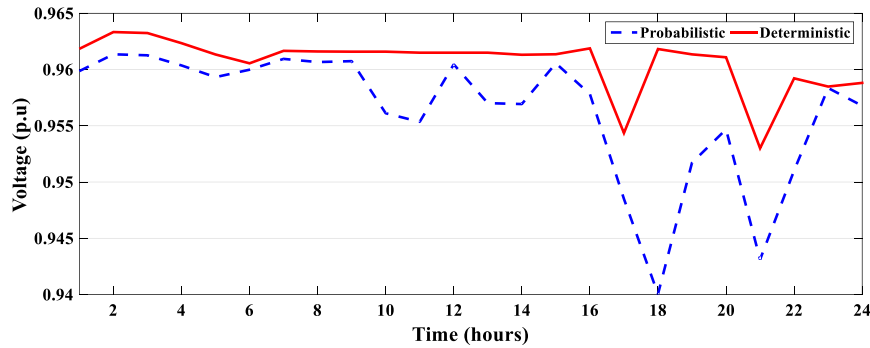

**Fig. 22.** *Comparison of probabilistic and deterministic modes (Bus 61).*
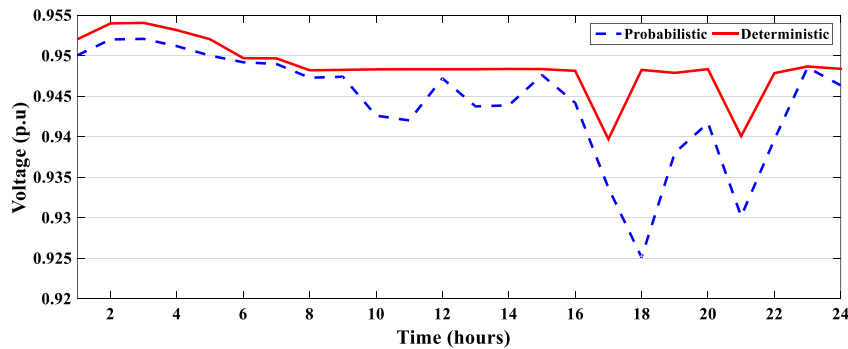
Fig. 23. *Comparison of probabilistic and deterministic modes (Bus 65).*

4.2.7. Processing details of the proposed algorithms

The VDI is expressed in percentage in Table 2 for some end buses. Bus 65 has a higher VDI than other buses in all methods, and in comparison between control methods, centralized control has a lower VDI for all buses. Among the two distributed control methods, the ADMM-based algorithm has a lower VDI than the DD-based algorithm, and with the addition of EVs, this index is decreased more than without them.

Table 2 VDI of end buses (%).

Bus number	Base Case	Centralized Control (without EV)	Distributed control algorithms			
			DD	ADMM	DD (with EV)	ADMM (with EV)
57	6.25	3.48	4.50	3.65	3.34	2.60
58	8.75	5.04	6.32	5.29	4.97	4.01
59	9.84	5.72	7.10	6	5.69	4.64
60	11.19	6.64	8.16	6.97	6.65	5.49
61	13.33	8.14	9.85	8.53	8.20	6.89
62	13.42	8.18	9.92	8.58	8.25	6.93
63	13.54	8.27	10	8.67	8.34	7.02
64	14.12	8.72	10.50	9.14	8.80	7.43
65	14.30	8.86	10.65	9.28	8.94	7.56

The processing details of the three voltage control methods are shown in Table 3. The problem-solving time and the number of iterations to reach convergence prove that the proposed ADMM-based algorithm reached convergence earlier than the proposed DD-based algorithm, and also the convergence speed is accelerated with the addition of EVs. The centralized control method has a lower AVDI than the other methods, and after that, the ADMM-based method and the DD-based method perform voltage improvement, respectively. The AVDI decreases in DD and ADMM methods with the addition of EVs. It should be noted that the centralized control method is without EVs. Therefore, the basis for comparing the centralized method with the proposed distributed algorithms should be in the case without EVs.

Table 3 Processing details of voltage control methods.

Processing Details	Base Case	Centralized Control (without EV)	Distributed control algorithms			
			DD	ADMM	DD (with EV)	ADMM (with EV)
Solving time (seconds)	-	234	119	95	93	80
Number of iterations	-	-	116	87	63	32
VDI of bus 65 (%)	14.3	8.86	10.65	9.28	8.94	7.56
AVDI (%)	2.55	1.29	1.85	1.33	1.18	0.91

Reduction of AVDI compared to the base case (%)	-	1.26	0.7	1.22	1.37	1.64
Reduction of AVDI compared to centralized control (%)	-	-	-0.56	-0.04	0.11	0.38
Total network losses (p.u)	0.280	0.167	0.207	0.177	0.160	0.145
Losses reduction rate compared to the base network (%)	-	40.30	26.23	36.63	42.83	48.11

5. Conclusion

This paper proposed DD-based and ADMM-based distributed methods in the presence of DERs and EVs. The proposed algorithms used the change of active and reactive power of DERs and the active discharge power of EVs for voltage control. The uncertainty of solar radiation and EVs' participation in each parking lot were modeled by the scenario-based method and 2PEM, respectively. This paper aimed to achieve a distributed control method in the presence of EVs that does not dependent on the central controller. In this regard, the centralized control method without the presence of EVs was modeled, and the results were compared. The simulation results were shown that the ADMM-based distributed control method has better results and higher convergence speed. Therefore, it enables the ability to implement operationally. On the other hand, the losses of the entire network were also reduced by improving the voltage in all methods.

6. References

[1] Mingxiang Zhou, Xing Li, Influence of green finance and renewable energy resources over the sustainable development goal of clean energy in China, Resources Policy, Volume 78, 2022.

[2] Momen, H., Abessi, A., Jadid, S., Shafie-khah, M., & Catalão, J. P. S. (2021). Load restoration and energy management of a microgrid with distributed energy resources and electric vehicles participation under a two-stage stochastic framework. International Journal of Electrical Power & Energy Systems, 133, 107320.

[3] Icaro Silvestre Freitas Gomes, Yannick Perez, Emilia Suomalainen, Rate design with distributed energy resources and electric vehicles: A Californian case study, Energy Economics, Volume 102, 2021.

[4] Jianyu Zhao, Xi Xi, Qi Na, Shanshan Wang, Seifedine Nimer Kadry, Priyan Malarvizhi Kumar, The technological innovation of hybrid and plug-in electric vehicles for environment carbon pollution control, Environmental Impact Assessment Review, Volume 86, 2021.

[5] Hemakumar Reddy Galiveeti, Arup Kumar Goswami, Nalin B. Dev Choudhury, Impact of plug-in electric vehicles and distributed generation on reliability of distribution systems, Engineering Science and Technology, an International Journal, Volume 21, Issue 1, 2018, Pages 50-59.

[6] Pirouzi, S., Aghaei, J., Niknam, T., Farahmand, H., & Korpås, M. (2018). Proactive operation of electric vehicles in harmonic polluted smart distribution networks. IET Generation, Transmission & Distribution, 12(4), 967–975.

[7] Partovi, M., Esmaeili, S., Aein, M.: Probabilistic optimal management of active and reactive power in distribution networks using electric vehicles with harmonic compensation capability. IET Gener. Transm.   Distrib. 16, 4304–4320 (2022).

[8] Kento Sasaki, Hirohisa Aki, Takashi Ikegami, Application of model predictive control to grid flexibility provision by distributed energy resources in residential dwellings under uncertainty, Energy, Volume 239,   Part B, 2022.

[9] Pasala Gopi, S. Venkat Rao, Ali Kimiyaghalam, Design of µ – controller for quarter electric vehicle with actuator uncertainties, Materials Today: Proceedings, Volume 60, Part 3, 2022, Pages 1927-1933.

[10] Qie Sun, Yu Fu, Haiyang Lin, Ronald Wennersten, A novel integrated stochastic programming information gap decision theory (IGDT) approach for optimization of integrated energy systems (IESs) with multiple uncertainties, Applied Energy, Volume 314, 2022.

[11] M. Aghamohamadi, A. Mahmoudi, and M. H. Haque, "Two-Stage Robust Sizing and Operation Co-Optimization for Residential PV-Battery Systems Considering the Uncertainty of PV Generation and Load," IEEE Trans. Ind. Informatics, vol. 17, no. 2, pp. 1005–1017, 2021.

[12] A. Baziar, R. Bo, M. D. Ghotbabadi, M. Veisi, and W. Ur Rehman, "Evolutionary Algorithm-Based Adaptive Robust Optimization for AC Security Constrained Unit Commitment Considering Renewable Energy Sources and Shunt FACTS Devices," in IEEE Access, vol. 9, pp. 123575-123587, 2021.

[13] S. Prajapati & E. Fernandez, "Performance Evaluation of Membership Function on Fuzzy Logic Model for Solar PV array," *2020 IEEE International Conference on Computing, Power and Communication Technologies (GUCON)*, 2020, pp. 609-613.

[14] M. N. Ali, K. Mahmoud, M. Lehtonen, and M. M. F. Darwish, "An Efficient Fuzzy-Logic Based Variable-Step Incremental Conductance MPPT Method for Grid-Connected PV Systems," in IEEE Access, vol. 9, pp. 26420-26430, 2021.

[15] Abolhassan Mohammadi Fathabad, Jianqiang Cheng, Kai Pan, Boshi Yang, Asymptotically tight conic approximations for chance-constrained AC optimal power flow, European Journal of Operational Research, 2022.

[16] Ke Li, Fan Yang, Lupan Wang, Yi Yan, Haiyang Wang, Chenghui Zhang, A scenario-based two-stage stochastic optimization approach for multi-energy microgrids, Applied Energy, Volume 322, 2022.

[17] Emrani-Rahaghi, P., Hashemi-Dezaki, H., & Hasankhani, A. Optimal stochastic operation of residential energy hubs based on plug-in hybrid electric vehicle uncertainties using two-point estimation method. *Sustainable Cities and Society,* Vol. 72, 2021, 103059.

[18] Ma, W., Wang, W., Chen, Z., & Hu, R. (2021). A centralized voltage regulation method for distribution networks containing high penetrations of photovoltaic power. *International Journal of Electrical Power & Energy Systems*, 129, 106852.

[19] Ji, H., Wang, C., Li, P., Zhao, J., Song, G., Ding, F., & Wu, J. (2018). A centralized-based method to determine the local voltage control strategies of distributed generator operation in active distribution networks. *Applied Energy*, 228, 2024–2036.

[20] Nowak, S., Wang, L., & Metcalfe, M. S. (2020). Two-level centralized and local voltage control in distribution systems mitigating effects of highly intermittent renewable generation. *International Journal of Electrical Power & Energy Systems,* 119, 105858.

[21] F. Rezaei, S. Esmaeili, Decentralized reactive power control of distributed PV and wind power generation units using an optimized fuzzy based method, *International Journal of Electrical Power & Energy Systems,* Vol. 87, pp. 27-42, 2017.

[22] D. I. Koukoula and N. D. Hatziargyriou, "Gossip algorithms for decentralized congestion management of distribution grids," IEEE Trans. Sustain. Energy, vol. 7, no. 3, pp. 1071–1080, 2016.

[23] H. Almasalma, J. Engels, and G. Deconinck, "Dual-decomposition-based peer-to-peer voltage control for distribution networks," CIRED - Open Access Proc. J., vol. 2017, no. 1, pp. 1718–1721, 2017.

[24] S. Magnusson, G. Qu, N. Li,. "Distributed optimal voltage control with asynchronous and delayed communication", IEEE Transactions on Smart Grid, vol.11, no.4, pp.3469-3482, 2020.

[25] Li, Z., Xu, Z., Xie, Y., Qi, D., & Zhang, J. (2021). Two-stage ADMM-based distributed optimal reactive power control method for wind farms considering wake effects. Global Energy Interconnection, 4(3), 251–260.

[26] Liao, W., Li, P., Wu, Q., Huang, S., Wu, G., and Rong, F. (2021). distributed optimal active and reactive power control for wind farms based on ADMM. *International Journal of Electrical Power & Energy Systems,* 129, 106799.

[27] Almasalma, H., Claeys, S., Deconinck, G.: 'Peer-to-peer-based integrated grid voltage support function for smart photovoltaic inverters', Applied Energy, vol. 239(1), pp. 1037–1048, 2019.

[28] Mohiti, M., Monsef, H., & Lesani, H. (2019). A decentralized robust model for coordinated operation of smart distribution network and electric vehicle aggregators. *International Journal of Electrical Power & Energy Systems,* 104, 853–867.

[29] Boyd S, Parikh N, Chu E, Peleato B, Eckstein J. "Distributed optimization and statistical learning via the alternating direction method of multipliers," Foundations and Trends®. Mach Learn 2011;3:1–122.

[30] X. Liu and S. Jia, "An Iterative Reputation Ranking Method via the Beta Probability Distribution," in IEEE Access, vol. 7, pp. 540-547, 2019.

[31] Kriegel, Hans-Peter*;* Schubert, Erich; Zimek, Arthur (2016). "The (black) art of runtime evaluation: Are we comparing algorithms or implementations?". Knowledge and Information Systems. 52 (2): 341–378.

[32] U. Agarwal, N. Jain, M. Kumawat & J. K. Maherchandani, "Weibull Distribution Based Reliability Analysis of Radial Distribution System with Aging Effect of Transformer," *2020 21st National Power Systems Conference (NPSC)*, 2020, pp. 1-6.

[33] Soroudi, A., & Amraee, T. (2013). Decision making under uncertainty in energy systems: State of the art. *Renewable and Sustainable Energy Reviews,* 28, 376-384.

[34] A. F Abdul Kadir, A. Mohamed, H. Shareef, & M.Z.C Wanik. (2013). Optimal placement and sizing of distributed generations in distribution systems for minimizing losses and THD_v using evolutionary programming. *Turkish Journal of Electrical Engineering and Computer Sciences*, 21, 2269-2282.

Figure captions

Fig. 1. *The proposed structure of a smart distribution network based on distributed voltage control.*

Fig. 2. *View of a simple distribution network in the presence of DERs and EVs.*

Fig. 3. *Flowchart of the proposed ADMM algorithm.*

Fig. 4. *IEEE 69-bus radial distribution system.*

Fig. 5. *The network load profile.*

Fig. 6. *61 bus voltage curve.*

Fig. 7. *65 bus voltage curve.*

Fig. 8. *61 bus voltage curve.*

Fig. 9. *65 bus voltage curve.*

Fig. 10. *61 bus voltage curve.*

Fig. 11. *65 bus voltage curve.*

Fig. 12. *DER4 Lagrangian multiplier curve.*

Fig. 13. *DER4 active and reactive power changes curve.*

Fig. 14. *Active power change curve of DER4 at 11:00.*

Fig. 15. *Reactive power change curve of DER4 at 11:00.*

Fig. 16. *61 bus voltage curve at 16:00.*

Fig. 17. *Total grid losses in 24 hours.*

Fig. 18. *61 bus voltage curve by implementing the DD algorithm.*

Fig. 19. *Total losses curve in 24 hours by implementing the DD algorithm.*

Fig. 20. *61 bus voltage curve by implementing the ADMM algorithm.*

Fig. 21. *Total losses curve in 24 hours by implementing the ADMM algorithm.*

Fig. 22. *Comparison of probabilistic and deterministic modes (Bus 61).*

Fig. 23. *Comparison of probabilistic and deterministic modes (Bus 65).*

Table captions

Table 1 Different scenarios in the case study.

Table 2 VDI of end buses (%).

Table 3 Processing details of voltage control methods.